

# Influence of Porosity on the Critical Currents of Trifluoroacetate-MOD $\text{YBa}_2\text{Cu}_3\text{O}_7$ Films

O. Castaño, A. Cavallaro, A. Palau, J. C. González, M. Rosell, T. Puig, S. Piñol, N. Mestres, F. Sandiumenge, A. Pomar, and X. Obradors

**Abstract**—The influence of porosity on the superconducting properties have been investigated on  $\text{YBa}_2\text{Cu}_3\text{O}_7$  thin films deposited on  $\text{LaAlO}_3$  (100) substrates by the so-called Trifluoroacetate (TFA) route. Micro-Raman spectroscopy have been used to determine the concentration of  $c$ -axis grains  $\delta$  in different samples and their influence on the final film porosity as observed from SEM imaging. This has been compared with measurements of resistivity and critical currents in the same samples. We prove that this  $\delta$  fraction is the main parameter controlling the porosity and hence the normal-state resistivity of the thin films. The optimization of the microstructure of these  $\text{YBa}_2\text{Cu}_3\text{O}_7$  TFA films allow to have high critical currents :  $J_c = 3 \times 10^6 \text{ A/cm}^2$  at 77 K.

**Index Terms**—Coated conductors, critical currents, superconducting thin films.

## I. INTRODUCTION

**E**X-SITU growth of  $\text{YBa}_2\text{Cu}_3\text{O}_7$  (YBCO) using trifluoroacetate (TFA) precursors is a very promising alternative for low cost fabrication of coated conductors [1]–[4]. One of its main advantages is that this route allow to grow pure YBCO phases at low reaction temperatures [1]. This is useful to avoid the formation of  $\text{BaCO}_3$  or any reaction with the buffer layers [5]–[8]. On the other hand, high critical currents in YBCO films are usually obtained at high reaction temperatures. Thus a major challenge to this route is to obtain critical currents as high as possible while keeping low reaction temperatures. This can not be achieved without a full control of the microstructural factors which may influence the film quality. However, and in spite of the numerous experimental efforts, there is still a lack of understanding of the influence of the different processing parameters on the final superconducting properties [2]–[4], [9]–[14].

In this work we have investigated the influence of growth conditions on the microstructure of YBCO thin films. In particular we will show that, in order to strongly reduce the porosity of the thin films, the  $c$ -axis grain growth should be enhanced. As a consequence superconducting properties, resistivity and critical current, will be dramatically improved.

Manuscript received August 5, 2002. This work was supported by the Spanish Science Ministry (MAT2001-1698 and 2FD97-1628), by the Generalitat of Catalunya (Catalan Pla de Recerca 00206) and the European Union through Marie Curie Program (HPMT-CT-2000-00106) and the Growth project SOLSULET (G5RD-CT-2001-00550).

The authors are with the Institut de Ciència de Materials de Barcelona, CSIC, Spain (e-mail: Xavier.obradors@icmab.es).

Digital Object Identifier 10.1109/TASC.2003.811832

## II. EXPERIMENTAL DETAILS

Samples are  $\text{YBa}_2\text{Cu}_3\text{O}_7$  thin films grown by spin coating stoichiometric trifluoroacetate precursor solutions onto (100)-oriented  $\text{LaAlO}_3$  substrates. Spinning rates (up to 6000 r.p.m.) and solution concentration (1.5 M) were chosen to obtain thin films of thickness in the order of 250 nm as determined from profile measurements and optical interferometric methods. After spinning the wet films were calcined in three steps: First, pyrolysis of the organic material was performed and films were heated up to 400 °C in a moist  $\text{O}_2$  atmosphere. Second, crystallization of YBCO films was done at high temperatures in a wet atmosphere with  $P(\text{H}_2\text{O}) = 73 \text{ mbar}$  and  $P(\text{O}_2) = 0.2 \text{ mbar}$ . The films were kept at high temperature just the time required for completing the reaction (typically one hour for  $T \sim 800^\circ\text{C}$ ) to avoid degradation after film growth due to the wet atmosphere. In this way, we can assume that the microstructural characteristics of the TFA films are mainly due to growth mechanisms directly related to temperature and atmosphere conditions of the reaction (thus, neglecting the influence of extra sintering time). Samples with different porosities were achieved by modifying reaction parameters as the temperature (from 700 to 830 °C) or the reaction atmosphere. Finally, films were oxidized at 450 °C in flowing  $\text{O}_2$  for 60 minutes.

Films were systematically characterized by X-ray diffraction, SEM and AFM after the different processing stages. Although more details will be given elsewhere [15] we should note that quality of the films strongly depends on the parameters controlling spin deposition and pyrolysis steps. Thus, these two processes were optimized in this work to avoid the formation of macrosegregations which could lead to the presence of secondary phases or to the degradation of epitaxy [15]. Qualitative information on the final porosity of the films was obtained from SEM imaging. Micro Raman spectroscopy ( $\lambda_L = 514.5 \text{ nm}$ ) allowed us to determine the orientation of the grains at a micrometric resolution (see below) [16]. Normal state dc transport properties were measured by a usual four-points technique. Critical currents were obtained from inductive measurements (SQUID magnetometer and ac third-harmonic susceptometer). The main error source affecting the absolute  $\rho(T)$  and  $J_c(T)$  values is due to uncertainties in the sample thickness and it is estimated to be of the order of 10-15%.

## III. RESULTS AND DISCUSSION

A comparison between two samples with different porosities is given in the SEM images of Fig. 1. Fig. 1(a) represents a

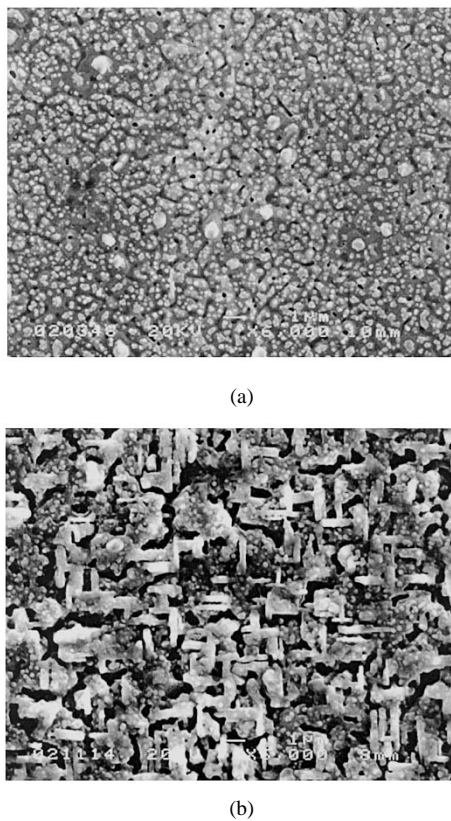


Fig. 1. SEM images of two YBCO thin films: (a) well densified, low porosity film and, (b) highly porous film. Note also the strong difference in the concentration of  $a/b$ -axis grains between both samples and how in (b) pores are mainly associated to these  $a$ -axis grains.

typical example of a well densified thin film. Here only some pores can be seen and a continuous and quietly uniform matrix is observed. Also, a few  $a/b$ -axis grains have been found with a typical size of  $1 \mu\text{m}$ . In contrast, SEM image of Fig. 1(b) illustrates the case of a high porous thin film. The differences between both pictures are evident. The two main features in Fig. 1(b) are the dominant presence of pores over the matrix and a huge difference in the relative proportion of  $a/b$ -axis oriented grains although the average size remains essentially unchanged ( $\sim 1 \mu\text{m}$ ). An interesting fact that we can observe from a careful looking at Fig. 1(b) is that pores seems to be always associated to the presence of  $a/b$ -axis oriented grains. To understand this we should keep in mind that the growth rate is much faster in the  $ab$ -planes than along  $c$ -direction. Thus when an  $a/b$ -axis grain nucleates it takes as much material as possible from the surrounding areas in order to increase its length perpendicular to the substrate. As a result there is a lack of material for the neighboring  $c$ -axis grains to fill the gap between  $a/b$  axis nucleation centers, and pores are thus formed. Therefore, in these TFA-YBCO samples it seems that the main factor controlling the porosity is the relative concentration of  $a/b$ -axis oriented grains. This concentration can be quantified from  $\mu$ -Raman spectroscopy measurements. The  $c$ -axis grain fraction  $\delta$  is given by the equation [17],

$$\delta = \frac{r(z_{Ag}^2 + x_{Ag}^2) - x_{B1g}^2}{r(z_{Ag}^2 - x_{Ag}^2) + x_{B1g}^2} \quad (1)$$

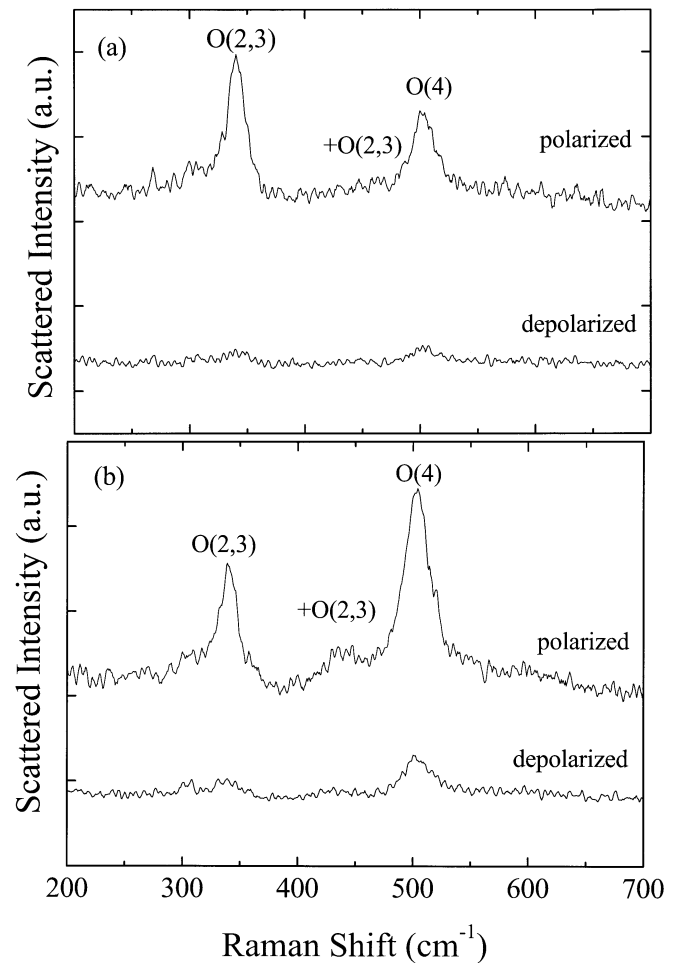


Fig. 2. Polarized and depolarized micro-Raman spectra of two typical regions: (a) with low porosity and small concentration of  $a/b$ -axis grains and (b) with high porosity and an important concentration of  $a/b$ -axis grains.

where  $z_{Ag}$ ,  $x_{Ag}$ ,  $x_{B1g}$  are the Raman tensor elements and  $r$  is the Raman intensity ratio  $r = I_{B1g}/I_{Ag}$  of the total intensities (i.e., the sum of the integrated Raman intensities in the polarized and depolarized spectra) of the O(2,3)- $B_{1g}$  and O(4)- $A_{1g}$  active modes observed at  $340 \text{ cm}^{-1}$  and  $500 \text{ cm}^{-1}$ , respectively. Fig. 2 shows two typical examples of the measured  $\mu$ -Raman spectra with a spot size of  $10 \mu\text{m}$ . Fig. 2(a) is a spectra taken in a region quite similar to that of Fig. 1(a) with almost no  $a/b$ -axis grains. The estimated  $c$ -axis fraction in this region was  $\delta \sim 0.9$ . In contrast, Fig. 2(b) represents a region similar to that of Fig. 1(b) with a higher presence of  $a/b$ -grains. In this case  $\delta$  was found to have a much lower value of  $\delta \sim 0.3$ . Although the precise dependence of this fraction  $\delta$  on the growth conditions deserves more experimental studies it seems that the temperature reaction and the  $P(\text{H}_2\text{O})$  of the reaction atmosphere are key factors. In particular we have systematically observed that, when keeping the others parameters constant, at higher reaction temperatures correspond higher values of  $\delta$  (i.e., less fraction of  $a/b$ -grains) and, consequently, lower porosities. Also, the quality of the wet films after spinning and pyrolysis steps seem to be crucial in the final morphology of the samples [15].

Now we will look at the influence of porosity on the normal state properties of the thin films. Fig. 3 shows the temperature

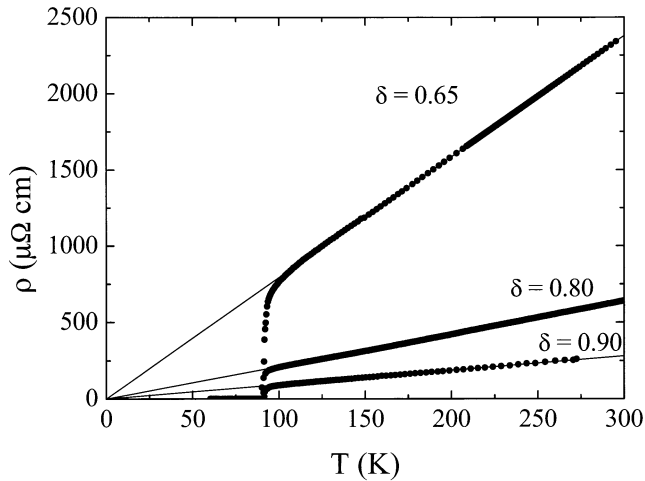


Fig. 3. Temperature dependence of the resistivity for three thin films with different  $c$ -axis grain fraction,  $\delta$ . Resistivity increases with the  $a/b$ -axis grain fraction, i.e., with higher porosities.

dependence of the resistivity  $\rho(T)$  for three thin films with different values of  $\delta$ . First, a normal-state linear behavior  $\rho(T) = \rho_0 + AT$  (solid lines in Fig. 3) with  $\rho_0 \approx 0$  is observed for all the samples here studied. As critical temperature value  $T_c = 90$  K indicates an optimal doping, this linearity suggests that electrical transport is only governed by the  $ab$ -planes and there is no out-of-plane or grain boundary contributions. This is in good agreement with the measured  $\delta$  values, above the percolation threshold for  $c$ -axis grains. These are typical features of high quality thin films such as those grown through vacuum processes [18], [19]. Second, the room temperature resistivity  $\rho(300\text{ K})$  increases when  $c$ -axis fraction  $\delta$  decreases. The lowest measured value  $\rho(300\text{ K}) \sim 200\ \mu\Omega\text{cm}$  is comparable with that obtained in YBCO single crystals [20], thus suggesting an almost pore-free sample. We may attribute this enhancement of the resistivity to a reduction of the effective cross section of the sample  $S_{ef}$  and, maybe most importantly, to an increase of the effective percolation length  $\ell_{ef}$  through the sample. The resistivity can be written as  $\rho(T) = (1/p)\rho_{ab}(T)$  where  $p$  is a parameter related to the porosity of the sample which depends on some function of the effective cross section and the percolation length,  $0 \leq p = f(\ell_{ef}, S_{ef}) \leq 1$ . We can deduce from Fig. 3 that  $p \sim 1$  for the sample with  $\delta = 0.9$  whereas it takes a value as low as  $p \sim 0.07$  for a sample with  $\delta = 0.65$ . This dependence of the room-temperature resistivity on the  $c$ -axis grain fraction is summarized in Fig. 4 for the samples here studied. Note that for each sample the given  $\delta$  value is an average of  $\mu$ -Raman spectra taken at different regions. The error bars reflect the dispersion between these spectra. It can be seen that there is a monotonous relationship between  $\delta$  and  $\rho(300\text{ K})$ . This confirms the results above commented on Fig. 1 and, in these samples, porosity is controlled by out-of-plane growth. Thus an improving scenario emerges from these results: A reduction of the porosity will lead to a direct and immediate enhancement of transport superconducting properties.

Finally, we have investigated the zero field critical current  $J_c$  in samples with different porosities. The temperature dependence of  $J_c$  for two of the samples of Fig. 3 is presented

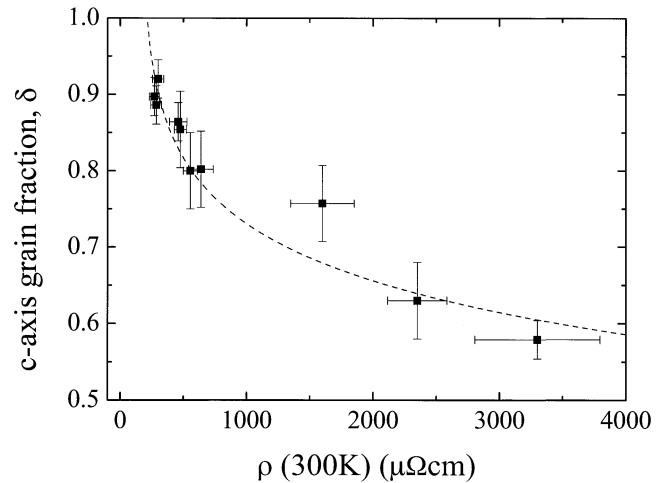


Fig. 4. Relationship between the measured room temperature resistivity,  $\rho(300\text{ K})$ , and the  $c$ -axis grain fraction,  $\delta$  calculated from  $\mu$ -Raman measurements for YBaCuO thin films with different porosities. Dashed line is a guide to the eye.

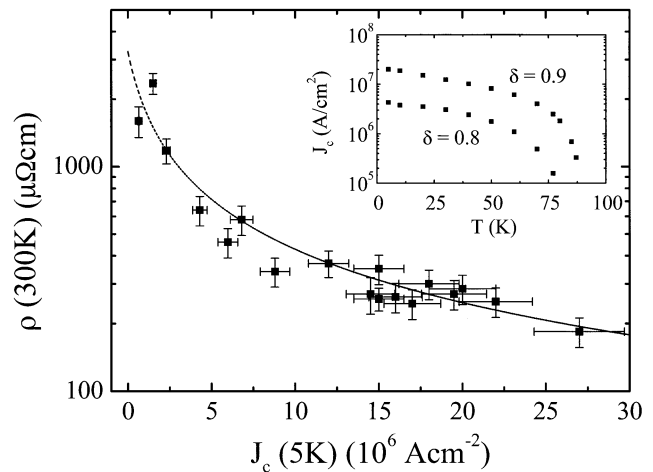


Fig. 5. Room temperature resistivity  $\rho(300\text{ K})$  as a function of the critical current  $J_c$  at 5 K for YBaCuO thin films with different porosities. Inset: Typical temperature dependence of the critical current  $J_c$  for two thin films with different  $c$ -axis grain fraction.

in the inset in Fig. 5. We can observe that the main difference between the samples is the absolute value of their critical current, being the temperature dependence quite similar. Furthermore, higher critical currents ( $J_c \sim 3 \times 10^6\text{ A/cm}^2$  at 77 K and  $J_c \sim 2 \times 10^7\text{ A/cm}^2$  at 5 K) were obtained for the less porous samples which as seen above also correspond to the less resistive samples. This close relationship between both quantities is illustrated in Fig. 5 where room temperature resistivity is represented as a function of the critical currents measured at 5 K for samples having a wide range of  $\delta$  (between 0.5 and 0.9) and, therefore, of porosities. This clear correlation suggests that the dominant factor of the degradation of the critical current in the more porous samples is the reduction of the effective cross section. However we can not neglect a contribution from the  $a$ -axis grains, especially in the samples where  $\delta$  is lower and it approaches the percolation threshold for the  $c$ -axis grains.

## IV. CONCLUSIONS

Growth of epitaxial YBa<sub>2</sub>Cu<sub>3</sub>O<sub>7</sub> thin films on single crystalline LaAlO<sub>3</sub> (100) substrates have been investigated using Trifluoroacetate precursors. The comparison of SEM imaging and micro-Raman spectroscopy indicates that the porosity observed in these as-grown films is mainly due to the presence of *a/b*-axis grains. These results suggest that the growth parameters should be optimized in order to favor *c*-axis growth and to keep the relative proportion of *a/b*-axis grains under control. This will lead to a drastically reduction of the porosity that it seems to be the main factor controlling the transport properties and therefore the critical currents in these as-grown TFA YBCO thin films.

## ACKNOWLEDGMENT

The authors acknowledge Servei de Microòpia Electrònica of Universitat Autònoma de Barcelona for the use of SEM facilities.

## REFERENCES

- [1] F. F. Lange, "Chemical solution routes to single-crystal thin films," *Science*, vol. 273, no. 5277, pp. 903–909, 1996.
- [2] A. Gupta, R. Jagannathan, E. I. Cooper, E. A. Giess, J. I. Landman, and B. W. Hussey, "Superconducting oxide films with high transition temperature prepared from metal trifluoroacetate precursors," *Appl. Phys. Lett.*, vol. 52, no. 24, pp. 2077–2079, June 1994.
- [3] P. C. McIntyre and M. J. Cima, "Heteroepitaxial growth of chemically derived *ex situ* Ba<sub>2</sub>YCu<sub>3</sub>O<sub>7-x</sub> thin films," *J. Mater. Res.*, vol. 9, no. 9, pp. 2219–2230, Sep 1994.
- [4] J. A. Smith, M. J. Cima, and N. Sonnenberg, "High critical current density thick MOD-derived YBCO films," *IEEE Trans. Appl. Supercond.*, vol. 9, no. 2, pp. 1531–1534, June 1999.
- [5] H. Fuji, T. Honjo, Y. Nakamura, T. Izumi, A. Takeshi, I. Hirabayashi, Y. Shiohara, Y. Iijima, and K. Takeda, "Deposition of CeO<sub>2</sub>/YSZ buffer layer on hastelloy substrates for MOD process of YBa<sub>2</sub>Cu<sub>3</sub>O<sub>7-x</sub> film," *Physica C*, vol. 357–360, no. 1-4, pp. 1011–1014, Aug 2001.
- [6] Y. Takahashi, T. Araki, K. Yamagiwa, Y. Yamada, S. B. Kim, Y. Iijima, K. Takeda, and I. Hirabayashi, "Preparation of YBCO films on CeO<sub>2</sub> buffered metallic substrates by the TFA-MOD method," *Physica C*, vol. 357–360, no. 1-4, pp. 1003–1006, Aug. 2001.
- [7] T. Araki, T. Yuasa, H. Kurosaki, Y. Yamada, I. Hirabayashi, T. Kato, T. Hirayama, Y. Iijima, and T. Saito, "High-*J<sub>c</sub>* YBa<sub>2</sub>Cu<sub>3</sub>O<sub>7-x</sub> films on metal tapes by the metalorganic deposition method using trifluoroacetates," *Supercond. Sci. Technol.*, vol. 15, no. 6, pp. L1–L3, June 2002.
- [8] M. Paranthaman, T. G. Chiralyil, S. Sathyamurthy, D. B. Beach, A. Goyal, F. A. List, D. F. Lee, X. Cui, S. W. Lu, B. Kang, E. D. Specht, P. M. Martin, D. M. Kroeger, R. Feenstra, C. Cantoni, and D. K. Chisten, "Fabrication of long lengths of YBCO coated conductors using a continuous reel-to-reel dip-coating unit," *IEEE Trans. on Applied Supercond.*, vol. 11, no. 1, pp. 3146–3149, March 2001.
- [9] P. C. McIntyre and M. J. Cima, "Microstructural inhomogeneities in chemically derived Ba<sub>2</sub>YCu<sub>3</sub>O<sub>7-x</sub> thin films: Implications for flux pinning," *J. Mater. Res.*, vol. 9, no. 11, pp. 2778–2788, Nov 1994.
- [10] T. Araki, H. Kurosaki, Y. Yamada, I. Hirabayashi, J. Shibata, and T. Hirayama, "Coating processes for YBa<sub>2</sub>Cu<sub>3</sub>O<sub>7-x</sub> superconductor by metalorganic deposition method using trifluoroacetates," *Supercond. Sci. Technol.*, vol. 14, no. 9, pp. 783–786, Sep 2001.
- [11] T. Araki, K. Yamagiwa, and I. Hirabayashi, "Fabrication of YBa<sub>2</sub>Cu<sub>3</sub>O<sub>7-x</sub> film by metalorganic deposition method using trifluoroacetates and its process conditions," *Cryogenics*, vol. 41, pp. 675–681, 2001.
- [12] L. Wu, Y. Zhu, V. F. Solovyov, H. J. Wiesmann, A. R. Moodenbaugh, R. L. Suenaga, and M. Suenaga, "Nucleation and growth of YBa<sub>2</sub>Cu<sub>3</sub>O<sub>7-x</sub> on SrTiO<sub>3</sub> and CeO<sub>2</sub> by a BaF<sub>2</sub> postdeposition reaction process," *J. Mater. Res.*, vol. 16, no. 10, pp. 2869–2884, Oct 2001.
- [13] H. Fuji, T. Honjo, Y. Nakamura, T. Izumi, A. Takeshi, I. Hirabayashi, Y. Shiohara, Y. Iijima, and K. Takeda, "Preparation of REBa<sub>2</sub>Cu<sub>3</sub>O<sub>7-x</sub> films grown by metal trifluoroacetate precursors," *Physica C*, vol. 357–360, no. 1-4, pp. 999–1002, Aug 2001.
- [14] M. P. Siegal, P. G. Clem, J. T. Dawley, R. J. Ong, M. A. Rodriguez, and D. L. Overmyer, "All solution chemistry approach for YBa<sub>2</sub>Cu<sub>3</sub>O<sub>7-x</sub>-coated conductors," *Appl. Phys. Lett.*, vol. 80, no. 15, pp. 2710–2712, Apr 2002.
- [15] O. Castaño, A. Cavallaro, A. Palau, J. C. González, M. Rosell, T. Puig, F. Sandiumenge, N. Mestres, S. Piñol, A. Pomar, and X. Obradors, "High quality YBa<sub>2</sub>Cu<sub>3</sub>O<sub>7</sub> thin films grown by trifluoroacetates metalorganic deposition," *Supercond. Sci. Technol.*, January 2003.
- [16] T. Puig, A. Puig-Molina, N. Mestres, H. Van Seijen, F. Alsina, J. C. González, X. Obradors, H. Graafsma, A. Usoskin, and H. C. Freyhardt, "Texture analysis of coated conductors by micro-Raman and synchrotron x-ray diffraction," *Mat. Res. Soc. Symp.*, vol. 659, pp. II5.6.1–II5.6.6, 2001.
- [17] N. Dieckmann, R. Kuersten, M. Loehndorf, and A. Bock, "Epitaxial quality of *c*-axis and *c*-axis oriented YBaCuO Films. Characterization by Raman spectroscopy," *Physica C*, vol. 245, pp. 212–218, 1995.
- [18] R. Wöndenweber, "Growth of high-*T<sub>c</sub>* thin films," *Supercond. Sci. and.*, vol. 12, pp. R86–R102, June 1999.
- [19] A. C. Westerheim, A. C. Anderson, D. E. Oates, S. N. Basu, D. Bhatt, and M. J. Cima, "Relation between electrical properties and microstructure of YBa<sub>2</sub>Cu<sub>3</sub>O<sub>7-x</sub> thin films deposited by single-target off-axis sputtering," *J. Appl. Phys.*, vol. 75, no. 1, pp. 393–403, Jan 1994.
- [20] T. Ito, K. Takenaka, and S. Uchida, "Systematic deviation from T-linear behavior in the in-plane resistivity of YBa<sub>2</sub>Cu<sub>3</sub>O<sub>7-y</sub>: Evidence for dominant spin scattering," *Phys. Rev. Lett.*, vol. 70, no. 25, pp. 3995–3998, June 1993.